


JUNE 18 2024

## Reducing contaminating noise effects when calculating low-boom loudness levels

Mark C. Anderson; Kent L. Gee ; J. Taggart Durrant; Alexandra Loubeau; William J. Doebler; Jacob Klos

 Check for updates

*J. Acoust. Soc. Am.* 155, 3889–3899 (2024)

<https://doi.org/10.1121/10.0026436>




**ASA**

Advance your science and career as a member of the **Acoustical Society of America**

[LEARN MORE](#)

## Reducing contaminating noise effects when calculating low-boom loudness levels

Mark C. Anderson,<sup>1,a)</sup> Kent L. Gee,<sup>1</sup>  J. Taggart Durrant,<sup>1</sup> Alexandra Loubeau,<sup>2</sup> William J. Doebler,<sup>2</sup> and Jacob Klos<sup>2</sup>

<sup>1</sup>Department of Physics and Astronomy, Brigham Young University, Provo, Utah 84602, USA

<sup>2</sup>Applied Acoustics Branch, NASA Langley Research Center, Hampton, Virginia 23681, USA

### ABSTRACT:

During NASA X-59 quiet supersonic aircraft community response tests, low-boom recordings will contain contaminating noise from instrumentation and ambient acoustical sources. This noise can inflate sonic boom perception metrics by several decibels. This paper discusses the development and comparison of robust lowpass filtering techniques for removing contaminating noise effects from low-boom recordings. The two filters are a time-domain Butterworth-magnitude filter and a frequency-domain Brick Wall filter. Both filters successfully reduce noise contamination in metric calculations for simulated data with real-world contaminating noise and demonstrate comparable performance to a modified ISO 11204 correction. The Brick Wall filter's success indicates that further attempts to match boom spectrum high-frequency roll-off beyond the contaminating noise floor are unnecessary and have marginal improvements on final metric calculations. Additionally, the Butterworth filter removes statistical correlation between ambient and boom levels for a real-world flight campaign, adding evidence that these techniques also work on other boom shapes. Overall, both filters can produce accurate metric calculations with only a few hundred hertz of positive signal-to-noise ratio. This work describes methods for accurate metric calculations in the presence of moderate noise contamination that should benefit X-59 and future low-boom supersonic aircraft testing.

© 2024 Acoustical Society of America. <https://doi.org/10.1121/10.0026436>

(Received 24 January 2024; revised 21 May 2024; accepted 27 May 2024; published online 18 June 2024)

[Editor: William James Murphy]

Pages: 3889–3899

### I. INTRODUCTION

Over the next several years, the National Aeronautics and Space Administration (NASA) will conduct supersonic aircraft flight tests for its Quesst Mission using the X-59 experimental aircraft. These tests will include sonic boom signature validation tests and, importantly, community noise tests.<sup>1–3</sup> The X-59 will be flown over several communities to gather both acoustic and human annoyance data. This will provide an opportunity to estimate test participant annoyance on the ground to provide recommendations for legislation to enable future low-boom aircraft to fly over land.<sup>4</sup> To do so, NASA has chosen several metrics that correlate with human annoyance.<sup>4–6</sup> These metrics will be calculated for sonic booms (or “thumps”) produced by the X-59 to determine noise acceptability in communities. The six metrics are a modified version of the Stevens Mark VII Perceived Level of Loudness (PL), the Indoor Sonic Boom Annoyance Predictor (ISBAP), and the A, B, D, and E-weighted Sound Exposure Levels (ASEL, BSEL, DSEL, ESEL).<sup>4,7,8</sup>

Because the X-59 aircraft can produce booms with low sound levels on the ground, NASA and contractors tasked with gathering acoustic data are left with the question of how to handle low signal-to-noise ratio (SNR) measurement environments.<sup>9</sup> As X-59 measurements will be deliberately made in urban environments, contaminating noise levels

will be higher than in most previous test campaigns, which happened primarily in quiet ambient environments, with a few exceptions.<sup>9–13</sup> Although overall contaminating noise levels can be somewhat predicted using geospatial data and machine learning,<sup>14,15</sup> exact levels during a recording cannot, making it impossible to know the exact effects of contaminating noise on recordings ahead of time.

References 16 and 17 show previous work on understanding contaminating noise effects and how to remove noise contamination in sonic boom metric calculations. Using the ISO 11204 standard as a framework,<sup>18</sup> additional, more aggressive, corrections were developed. The best results were obtained by using the “Custom E” and “Custom F” corrections discussed in Ref. 17. These corrections successfully reduced the amount of noise contamination in metric calculations. Although this method appears to be largely successful, it is useful to investigate other methods that are also easily implemented. Using multiple methods can provide a way to validate the results.

Considering the amount of data that will be generated by X-59 testing, it is important to have a method for quickly and accurately removing noise contamination from recordings. The number of anticipated measurements for every boom is expected to be more than 100 because noise monitors will be spaced throughout the community and surrounding areas,<sup>16</sup> and if a simple yet effective method for removing noise contamination can be implemented then overall effort and data analysis cost may be reduced.

<sup>a)</sup>Email: mark.anderson@byu.net

The remainder of this paper proceeds as follows. Section II contains the process and theory behind creating filters for removing contaminating noise. Section III discusses the required cutoff frequency for accurate metric calculations within  $\pm 1$  dB of a perfectly clean waveform when the contaminating noise is perfectly defined. Section IV then applies these filters to more realistic simulations. Following that, Section V includes a direct comparison between the Butterworth, Brick Wall, and ISO 11204 filters. Section VI demonstrates that the Butterworth filter successfully removes statistical correlation between ambient and boom PL values in a real-world measured dataset, suggesting that the Butterworth filter can be useful for different-shaped booms. Overall, both the Butterworth and Brick Wall filters successfully reduce noise contamination, and therefore, reduce the total effective measurement cutoff frequency required for accurate metric calculations.

## II. FILTERING TECHNIQUES

This paper presents two low-pass filters for high-frequency contaminating noise removal. The first is a time-domain zero-phase filter with sixth-order Butterworth filter magnitude response, hereafter referred to simply as the “Butterworth” filter. This filter is implemented via the MATLAB *butter* and *filtfilt* commands.<sup>19</sup> The *butter* command is used to generate a third-order filter, which is used as the input to the *filtfilt* command which applies the filter both forward and backward, producing zero phase distortion and doubling the final filter order to sixth order. The second filter presented in this paper is a purely frequency-domain filter that is referred to as the “Brick Wall” filter. This filter simply discards all frequency data above a selected one-third octave (OTO) band and serves as a limiting case to help determine whether there are possible benefits of investigating other filter shapes.

To determine filter effectiveness on low-boom recordings, this paper uses a dataset of simulated low-boom recordings from the X-59, which consists of predicted sonic boom ground signatures from a previous X-59 design iteration identified as “C609.”<sup>20</sup> These simulations include propagation of the C609 near-field pressure through realistic atmospheric profiles without turbulence effects. The dataset is a random sample of the low booms produced in Ref. 21. These waveforms have been resampled to a sample rate of 51.2 kHz and have been padded with zeros so that the peak pressure occurs at 0.1 s and the total waveform is 650 ms long. To simulate contaminating noise effects on these recordings, measured ambient recordings were used from the Quiet Supersonic Flights 2018 (QSF18) test campaign,<sup>11,13</sup> and superposed on the X-59 simulations. For this measurement campaign, data were recorded in Galveston, TX and the contaminating noise recordings are used here to simulate X-59 recordings in community environments. Because the analyses within this paper are largely limited to simulated C609 waveforms with measured QSF18 ambient noise recordings, the results may not fully generalize to

other waveform shapes and ambient noise environments. However, these methods are shown to work well on measured QSF18 sonic booms in Sec. VI, supporting the claim that these methods may be applicable to other sonic boom shapes.

The following discussion consists of a filtering analysis walk-through example. Figure 1(a) shows a C609 waveform both before and after contaminating noise from QSF18 is added. These waveforms are hereafter referred to as the “clean” and “noisy” waveforms, respectively. Spectra for the clean and noisy booms are shown in Fig. 1(b), alongside the spectrum for the contaminating noise. All results in this paper use a 650-ms recording for both the contaminating noise and the sonic boom. The spectra were calculated using a tapered cosine window with a cosine fraction of 0.1. Longer contaminating noise recordings could be used to estimate the contaminating noise spectrum if the ZSEL spectra for the boom and the noise are properly scaled to account for different recording durations. Because this is a simulation, the contaminating noise is perfectly known, and an independent spectrum can be produced. At low frequencies, the noisy recording is dominated by the sonic boom and at high frequencies is dominated by contaminating noise. An important metric for the noisy sonic boom is the frequency-dependent SNR, defined as

$$\text{SNR}(f) = \text{ZSEL}_{\text{boom}}(f) - \text{ZSEL}_{\text{ambient}}(f) \quad (1)$$

and plotted as a function of frequency in Fig. 1(c), where  $\text{ZSEL}(f)$  is the flat-weighted sound exposure level spectrum. The key takeaways from this figure are that the highest SNR values occur around or below 10 Hz for this recording and that contaminating noise completely overwhelms the recording at frequencies greater than about 600 Hz. Because most of the metrics are impacted more by frequencies in the hundreds of hertz range than in the tens of hertz range, this paper focuses on removing the high-frequency noise. This work could potentially be combined with the wind noise removal techniques found in Ref. 22 to reduce any contamination due to wind noise at low frequencies. Results in this paper indicate that focusing only on high frequencies performs remarkably well.

The process for implementing the filter is as follows:

- (1) Calculate the SNR spectrum using Eq. (1) as shown in Fig. 1(c).
- (2) Determine the first OTO band center frequency with an SNR below a chosen threshold. This frequency becomes known as the “cutoff frequency” This paper uses a threshold of 3 dB.
- (3) Set that OTO band center frequency to be the filter cutoff frequency.
- (4) Apply the filter to the waveform (Butterworth) or spectrum (Brick Wall). The resultant spectra are shown in Fig. 2. For the Brick Wall filter, simply discard all OTO band spectral data above this cutoff frequency, keeping the value at the cutoff frequency itself. For example, if the SNR drops below 3 dB between 250 and 315 Hz, the

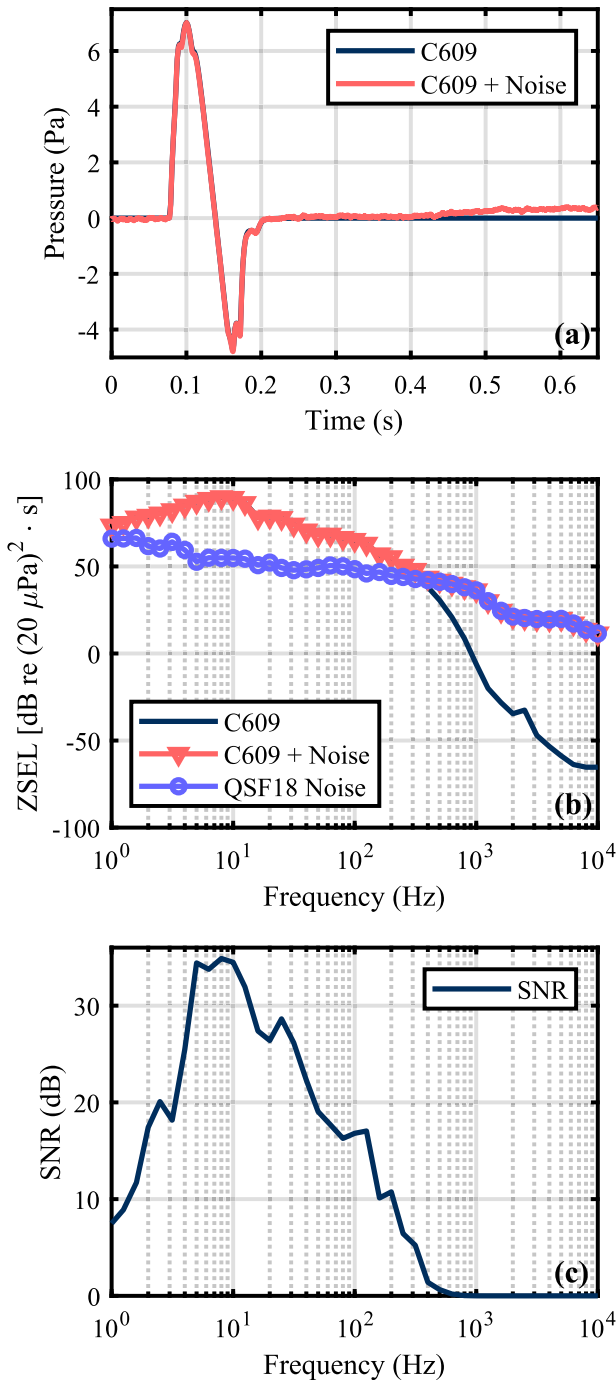


FIG. 1. (Color online) (a) An example simulated C609 waveform with and without added contaminating noise. (b) The OTO band spectra for the waveforms. Also, included is the contaminating noise that was added to the clean boom to produce the noisy boom. (c) The signal-to-noise ratio for the noisy boom (C609 + Noise) relative to the contaminating noise (QSF18 Noise).

cutoff frequency is 250 Hz. Spectral data corresponding to 315 Hz and above are discarded, while data at 250 Hz and below are kept.

Note that other filter designs and filter orders may yield acceptable or even better results. An exhaustive search of filters and orders was not performed, and the Brick Wall filter results throughout the remainder of this paper

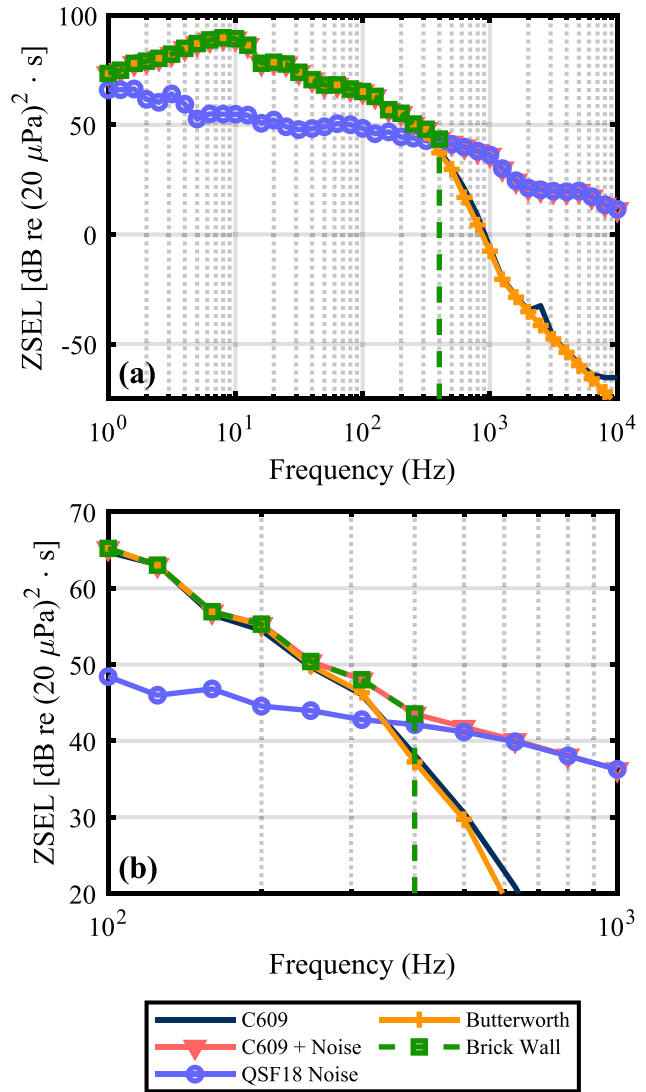


FIG. 2. (Color online) The combined spectra. Notice that for this boom the Butterworth filter follows the high-frequency roll-off closely. (a) The full spectra. (b) The zoomed-in spectra. Notice that the Brick Wall filter keeps the value associated with the cutoff frequency of 400 Hz, removing all data above the cutoff frequency but not at the cutoff frequency itself.

demonstrate that precisely matching the spectral shape is not important for accurate metric calculations.

Note also that many booms suffer from low-frequency contamination that tends to be at frequencies unimportant to most metrics but may cause the filter to be applied at an unnecessarily low frequency. To avoid this, all results in this paper use a minimum allowable cutoff frequency of 50 Hz, and if the low-SNR threshold was crossed before 50 Hz, then the cutoff frequency was set to the first frequency greater than 50 Hz for which the SNR threshold was crossed. The work of Ref. 22 may be useful in the future to remove this constraint.

Another important set of visualizations when calculating sonic boom metrics are the loudness curves produced during the PL calculation. These curves are shown in Fig. 3 both with and without the filtered spectra. In Fig. 3(a), we see that the frequencies for which these sonic booms have

their peak SNR [as shown previously in Fig. 1(c)] are not the frequencies that contribute most to loudness, but rather the frequencies around 100 Hz. This is important because it means that the frequencies that are the most impactful for calculating the PL have lower SNR values, increasing the likelihood of metric inflation due to contaminating noise. In Fig. 3(b), we see the same loudness curves, but with the two filtered results overlaid, showing how both filters reduce noise contamination at high frequencies. It is important to note that the standard PL calculation for sonic booms uses a correction designed specifically for sonic booms that accounts for two shocks in the waveform.<sup>8</sup> Although it is currently standard practice to use this same correction when calculating the PL for a sonic boom and its surrounding contaminating noise,<sup>9</sup> its appropriateness for contaminating noise levels is not well-understood. To stay consistent with the literature,<sup>9,11</sup> this paper uses the current standard practice of applying this correction to the boom and ambient PL

metrics; however, the correction's applicability to contaminating noise and sonic booms that do not match the assumptions made in Ref. 8 warrants future analysis.

Once the lowpass filter has been applied, we can compare the metric values for the clean, noisy, and filtered C609 simulations. Table I shows these results for the example boom discussed in Figs. 1–3. Notice that the noisy boom tends to have inflated metric values due to the addition of contaminating noise, especially for the PL, ISBAP, and ASEL. Both filters reduce the contaminating noise impact and show good agreement with the clean metric values. Also, both filters produce the same final metric values within 0.2 dB. This demonstrates that both filters are approximately equally effective for this boom. Note also that several metrics are essentially unaffected by the contaminating noise.

### III. RESULTS WITH KNOWN CONTAMINATING NOISE

The same analysis described above was applied to a set of 300 similar simulations using the C609 simulations and real-world contaminating noise. Each boom was randomly paired with ambient data recorded at QSF18 and was analyzed 30 times with different contaminating noise recordings drawn from a bank of 5081 potential 650-ms recordings. Because contaminating noise recordings were randomly selected, there were a few repeated combinations. The duplicates were removed, and, in the end, there were 8973 unique pairings of boom and ambient recordings. Analyses were performed exactly as discussed above, with the contaminating noise being perfectly known for each recording. Section IV discusses applications to simulated data where the contaminating noise is not perfectly defined.

Two metrics are shown in detail here: PL and BSEL. The results for both metrics are shown in Fig. 4. In each subplot, all booms are represented exactly once as a function of their individual cutoff frequency on the abscissa. The ordinate contains the change in metric value relative to the clean, no-noise-added boom. The following labels are useful for this figure and throughout the following discussions:

$$\Delta PL_{n-c} = \text{noisy PL} - \text{clean PL}, \tag{2}$$

$$\Delta PL_{f-c} = \text{filtered PL} - \text{clean PL}, \tag{3}$$

$$\Delta PL_{n-f} = \text{noisy PL} - \text{filtered PL}. \tag{4}$$

In subplot (a), the difference created by applying the contaminating noise to the clean boom is shown. For example, if the clean PL of the simulated boom is 75 dB, but adding noise creates a PL of 78 dB and reduces the boom cutoff frequency to 400 Hz, then a single dot is placed on this subplot at (400 Hz, 3 dB). The process is repeated for all boom and noise realizations. The result is 8973 data points segregated by cutoff frequency. Therefore, a distribution of  $\Delta PL$  values exists at each frequency band and some statistical results are shown on the plot at each band. The green bars denote plus and minus two standard deviations from the

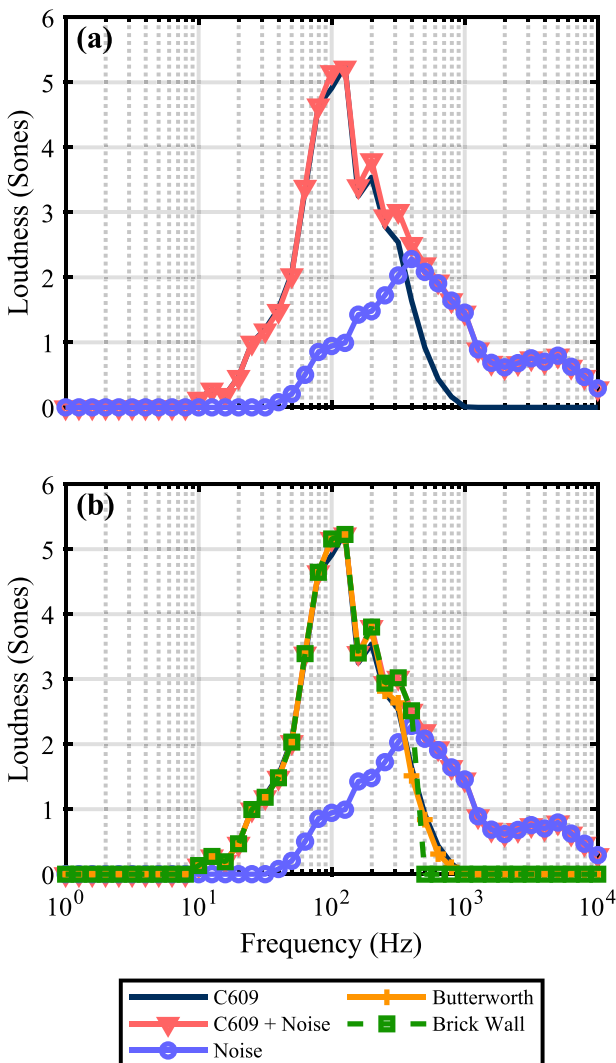


FIG. 3. (Color online) (a) Loudness spectra for the original C609 recording, the C609 recording with contaminating noise, and the contaminating noise on its own. (b) The same loudness spectra as (a), but the loudness spectra of the C609 recording with contaminating noise has been filtered according to the Butterworth and Brick Wall methods and shown.

TABLE I. The metric calculations for the simulated C609 walk-through example shown in Sec. II. Notice that both the Butterworth and Brick Wall filters can reduce the noise contamination to better-approximate the metrics from the clean recording. Although not considered part of the candidate metrics for sonic booms, CSEL and ZSEL are included for completeness. All values are shown in decibels.

	Clean value	Noisy value		Butterworth filter result		Brick wall filter result	
		Result	Difference	Result	Difference	Result	Difference
PL	66.6	69.6	3.0	66.6	0.0	66.7	0.1
ISBAP	78.9	81.5	2.6	78.9	0.0	78.9	0.0
ASEL	53.1	54.0	0.9	53.3	0.2	53.5	0.4
BSEL	68.0	68.1	0.1	68.1	0.1	68.1	0.1
CSEL	82.4	82.4	0.0	82.4	0.0	82.4	0.0
DSEL	70.6	70.7	0.1	70.6	0.0	70.6	0.0
ESEL	63.4	63.7	0.3	63.6	0.2	63.6	0.2
ZSEL	96.7	96.6	-0.1	96.6	-0.1	96.6	-0.1

mean value of the distribution and the blue bars denote the 95% confidence interval for the mean value of the distribution. These statistics help to visualize the spread and number of data points at each frequency. Subplot (b) shows the same type of plot for the BSEL metric. Notice that the BSEL is substantially less affected by contaminating ambient or instrumentation noise than the PL. Subplot (c) shows the PL results again, but after applying the Butterworth filter to the noisy booms. Notice that after applying this filter, the mean values tend to lie much closer to 0 dB and the standard deviation bars have become smaller. This indicates that, although there is still spread in the data, the mean PL values calculated after applying the Butterworth filter are much closer to the benchmarks. Subplot (d) shows the same for BSEL and subplots (e) and (f) represent the same results using the Brick Wall filter instead.

From Fig. 4, the required cutoff frequency for accurate metric calculations can be estimated. The estimate is obtained by determining the required cutoff frequency for the mean plus or minus two standard deviations to lie within  $\pm 1$  dB of the corresponding metric for the clean boom. Graphically, this is the required cutoff frequency such that the green bars do not stray beyond  $\pm 1$  dB, and this analysis can be performed for the unfiltered case as well as the two filtered cases. This produces the results shown in Table II, and a few of the results can be compared visually with Fig. 4. Each row indicates results for a given metric, shown in the left-most column. Results were truncated at 50 Hz because that was the minimum allowed cutoff frequency. A primary result from this table is that both the Butterworth and Brick Wall filters successfully reduced the cutoff frequency required for good metric agreement with the clean booms. Another important result is that there is little difference between the required cutoff frequencies for the two types of filters. The choice of  $\pm 1$  dB is arbitrary and other criteria could certainly be chosen. It should be noted that although nearly 10 000 realizations were used, the cutoff frequency values listed in Tables II and III may change a little depending on the simulation details. Such appears to be the case for the ZSEL metric, which shifts from 160 Hz in Table II across all three columns to 125 Hz in Table III (in Sec. IV) across all three columns, a change of one

third-octave band. Despite this small change that can occur for the recommended cutoff frequencies, the trends remain intact, and the cutoff frequencies do not vary dramatically between simulations.

The fact that the ZSEL metric requires a higher cutoff frequency than the CSEL metric can be explained by the presence of low-frequency noise sources like wind noise, which corrupt the ZSEL metric more than the CSEL metric. Thus, for applications where the ZSEL is important, low-frequency noise reduction should be considered. For wind noise reduction, the work in Ref. 22 may be useful. As both the CSEL and ZSEL metrics are not in the list of NASA human-perception metrics,<sup>4</sup> having been included within this paper for completeness only, these interesting results may not be a primary concern for the upcoming X-59 community flight tests.

These results indicate that both the Butterworth and Brick Wall filters can be used for accurate sonic boom metric calculations using the current metrics and when high-frequency noise is the dominant contaminating noise source.

#### IV. FILTER APPLICABILITY TO MORE-REALISTIC SIMULATIONS

##### A. Contaminating noise stationarity

If the contaminating noise is not stationary over short intervals, then attempting to remove contaminating noise becomes more challenging. It is therefore relevant to consider the question of how stationary the contaminating noise is over short intervals. To investigate this, 2383 contaminating noise recordings from QSF18 of duration 1300 ms were used to determine spectral differences between the first and second halves of the recordings. These recordings were created using the channels with the lowest instrumentation noise at the four stations that recorded about one minute of ambient noise before each sonic boom measurement. These four stations are discussed further in Ref. 13. Results are shown in Fig. 5. At frequencies below about 20 Hz, there is much more variability between recording halves, perhaps due to wind noise. However, the high SNR during most sonic boom recordings at those frequencies means that this is unlikely to substantially impact metric calculations.

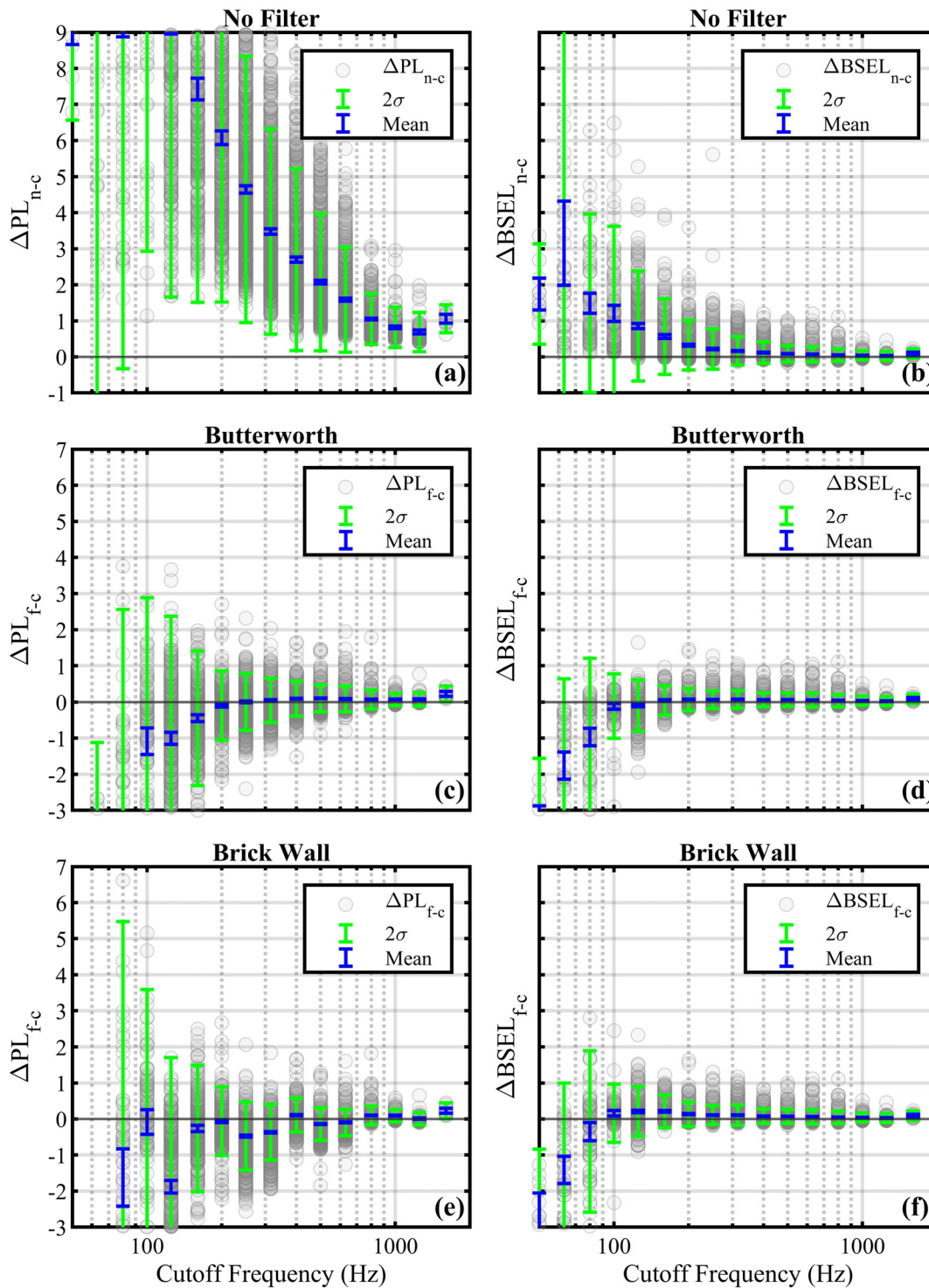


FIG. 4. (Color online) The difference, relative to the clean boom, as a function of the cutoff frequency. (a) The unfiltered PL value (dB) minus the clean boom PL (dB). The difference is denoted by  $\Delta PL_{n-c}$  where the quantity “n-c” denotes “noisy minus clean.” The circles represent individual boom realizations, so there are a total of 8973 circles on this plot. Green bars denote two standard deviations for the distribution at each frequency. Blue bars denote the 95% confidence interval for the mean value of the distribution at each frequency. (b) Same, but for the BSEL metric. (c) The same results for PL, but after applying the Butterworth filter. The quantity  $\Delta PL_{f-c}$  denotes “filtered minus clean.” (d) Same, but for the BSEL metric. (e) Same, but for the PL metric using the Brick Wall filtering technique. (f) Same, but for the BSEL metric.

**B. Mock recordings**

Table II described the necessary cutoff frequency for accurate metric calculations when contaminating noise during the boom recording is perfectly known. To better

simulate a real-world recording where contaminating noise is known only before the boom (i.e., “preboom ambient”), a 1300-ms recording of contaminating noise is added to each 650-ms boom with the boom in the second half of the

TABLE II. The results of using different filtering techniques on the minimum cutoff frequency required for accurate metric calculations within 1 dB, defined as the mean  $\pm$  two standard deviations. These results are for the case that the contaminating noise is perfectly known. Frequencies are the OTO band center frequencies.

	Unfiltered (Hz)	Butterworth filter (Hz)	Brick Wall filter (Hz)
PL	>1600	250	400
ISBAP	>1600	200	400
ASEL	800	200	250
BSEL	250	125	100
CSEL	50	50	50
DSEL	200	100	80
ESEL	500	160	160
ZSEL	160	160	160

recording. An example of this is shown in Fig. 6. Therefore, only the 650 ms of contaminating noise immediately preceding the boom is known, and the 650 ms of contaminating noise during the boom can only be estimated, which is more typical of real-world measurements.<sup>9</sup> These types of waveforms are referred to hereafter in this paper as “mock recordings.”

To simulate a real-world measurement, 8956 unique mock recordings were created by randomly pairing the 300 C609 booms with 1300-ms segments from contaminating noise recordings from four stations at QSF18.<sup>11,13</sup> Contaminating noise before the boom was used to estimate the SNR during the boom, and the filters were applied. Results are shown in Table III. Several metrics show that a higher cutoff frequency is required for accurate metric estimations relative to the case where contaminating noise is perfectly known (Table II), following from the increased uncertainty in contaminating noise levels during the recording. This is further illustrated in Fig. 7, which shows the same type of results as Fig. 4, but using these mock recordings, where the noise during the sonic boom is not perfectly known, only estimated. Notice the increase in the uncertainty when the contaminating noise is not perfectly known. Experience shows that the recommendations in Table III may drift by a couple bands between different simulations, though the trends remain intact.

TABLE III. Results of using different filtering techniques on the minimum cutoff frequency required for accurate metric calculations (mean  $\pm$  2 standard deviations) within 1 dB. These results are for the case that the contaminating noise is not perfectly known but is estimated by using the 650 ms before the boom.

	Unfiltered (Hz)	Butterworth filter (Hz)	Brick Wall filter (Hz)
PL	>1600	400	400
ISBAP	>1600	400	400
ASEL	1000	400	400
BSEL	200	125	100
CSEL	50	50	50
DSEL	160	100	80
ESEL	500	160	200
ZSEL	125	125	125

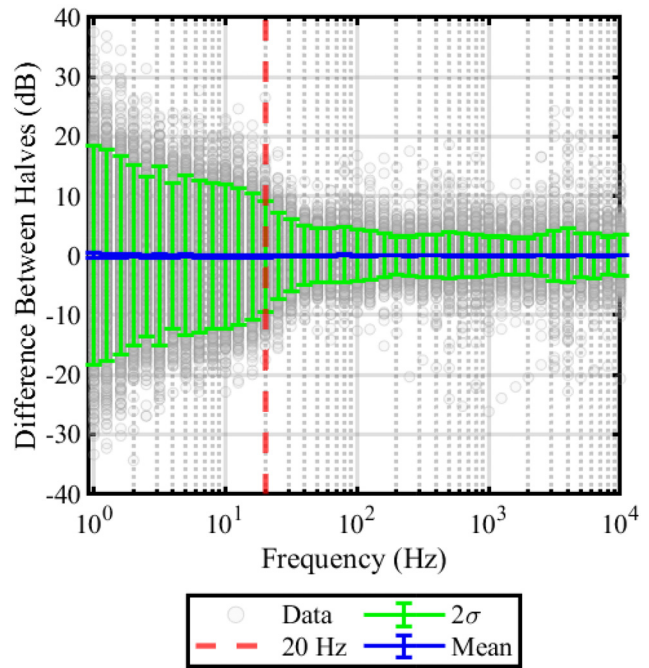


FIG. 5. (Color online) Analysis of contaminating noise variability at QSF18. Levels at frequencies below about 20 Hz can change much more than levels at higher frequencies over the course of 1300 ms.

### V. COMPARISON WITH ISO 11204

How does this filtering technique compare with other state-of-the-art techniques? A popular technique for reducing contaminating noise corruption is to use a spectral subtraction method,<sup>9,17</sup> such as that used in ISO 11204.<sup>18</sup> A spectral subtraction method takes the preboom ambient and boom spectra and subtracts them on an energy basis before calculating metrics. A revised, more aggressive, formulation

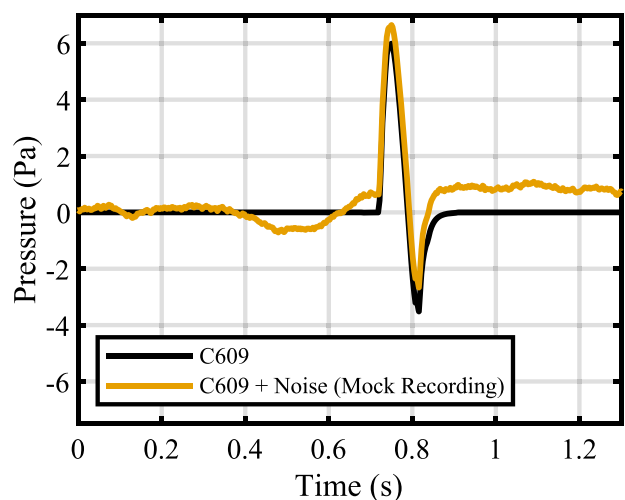


FIG. 6. (Color online) An example mock recording. A 1300-ms contaminating noise recording is combined with the clean boom. This results in 650 ms of contaminating noise before the boom window, allowing for analyses to be performed that use the first 650 ms of contaminating noise to estimate contaminating noise during the actual boom event. This is more realistic because the contaminating noise during the boom is not able to be perfectly known.



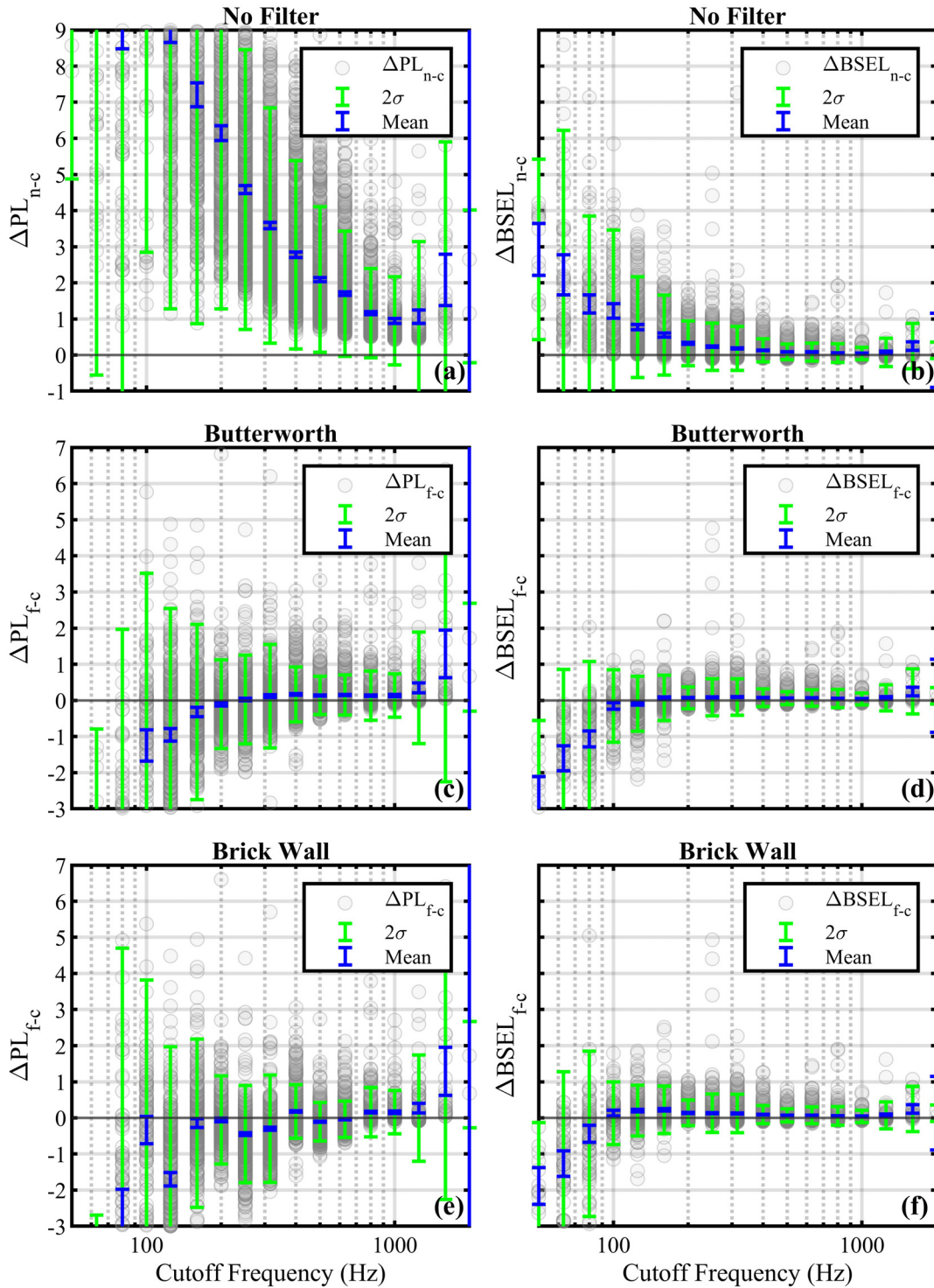


FIG. 7. (Color online) The difference, relative to the clean boom, as a function of the cutoff frequency. (a) The unfiltered PL value (dB) minus the clean boom PL (dB). The difference is denoted by  $\Delta PL_{n-c}$  where the quantity “n-c” denotes “noisy minus clean.” The circles represent individual boom realizations, so there are a total of 8956 circles on this plot. Green bars denote two standard deviations for the distribution at each frequency. Blue bars denote the 95% confidence interval for the mean value of the distribution at each frequency. (b) Same, but for the BSEL metric. (c) The same results for PL, but after applying the Butterworth filter. The quantity  $\Delta PL_{f-c}$  denotes “filtered minus clean.” (d) Same, but for the BSEL metric. (e) Same, but for the PL metric using the Brick Wall filtering technique. (f) Same, but for the BSEL metric.

of ISO 11204 can be found in Ref. 17 and the revised filters recommended in that work are the “Custom E” and “Custom F” corrections. The Brick Wall and Butterworth filters proposed in this paper are directly compared against

these two modified ISO 11204 corrections, where the same 8956 mock recordings were used from Sec. IV. The differences between the filtered mock recording and the clean boom PL values ( $\Delta PL_{f-c}$ ) were calculated and are shown in

Fig. 8 and a few statistics for the distributions are shown in Table IV. Subplot (a) shows only the results using the ISO 11204 adaptations. Subplot (b) superimposes the results from the methods proposed in this paper.

Notice that all four methods produce similar results, with the methods produced in this paper perhaps slightly outperforming the ISO 11204-based methods by producing more values near  $\Delta PL_{f-c} = 0$  dB. However, based on this analysis alone, none of these methods stand out as a clear choice. It is possible that additional simulations and measurements will determine the best approach to contaminating noise mitigation. These methods should all continue to be studied once real low-boom measurements are available, and we should be careful not to draw final conclusions based on simulated results that may work great for particular simulations but not fully generalize to other sonic booms and ambient noise environments. It is possible that during X-59 testing, multiple methods should be used in tandem to help estimate uncertainty in the final metric values. It is likely that the ISO 11204-based methods will outperform the methods presented in this paper when the contaminating noise is tonal. However, because the Butterworth filter is a time-domain technique, it could possibly be used to produce waveforms with reduced high-frequency noise contamination.

**VI. REDUCING STATISTICAL CORRELATION BETWEEN SIGNAL AND CONTAMINATING NOISE**

An important consideration for this work is whether the methods presented in this paper are useful for real-world measurements and waveforms that do not have the same shape as the C609 simulations. Because real-world measurements do not have known “clean” metric values, determining whether a method successfully removes the contaminating noise cannot be demonstrated exactly. However, it can be investigated statistically. A linear fit can be created for the data both before and after contaminating noise removal, returning an estimated slope and a p-value associated with that slope. Figure 9 shows the result of such an analysis on the QSF18 dataset. This dataset consists of sonic booms produced by an F-18 aircraft performing a low-boom dive maneuver about 20 miles off the coast of Galveston, TX.<sup>11,13</sup> In total, 379 boom PL values from QSF18 are plotted as a function of the corresponding ambient PL. Sonic booms with a cutoff frequency less than or equal to 50 Hz were omitted, as those are likely too contaminated to acquire accurate metric calculations. Figure 9(a) shows the unfiltered boom results. There is a clear trend for the boom PL to be greater if the ambient PL is also greater. The red line indicates the fitted linear model. Note that the p-value is  $2.71 \times 10^{-9}$ , indicating a strong statistical relationship between the ambient and boom PL values (i.e., a strong likelihood of a nonzero fitted slope). The almost perfectly straight lower boundary in the scattered data results from the boom PL being limited to the ambient PL, creating an effective floor for the PL metric. This is visualized by adding the blue line, which represents a one-to-one

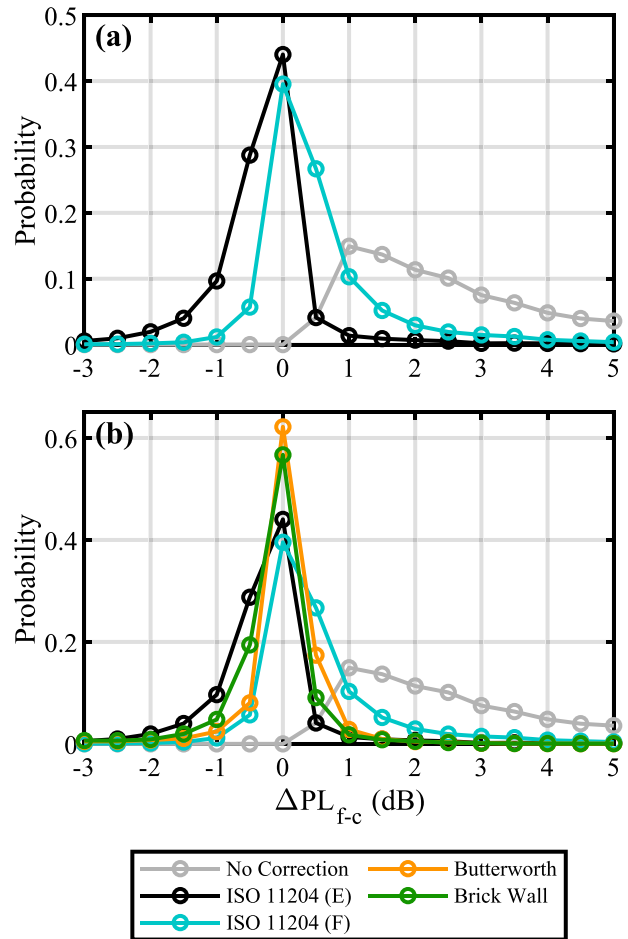


FIG. 8. (Color online) Comparison with the ISO 11 204-based methods. (a) The distribution of filtered metrics relative to the clean boom. (b) Same distributions, but with the methods proposed in this paper included.

relationship between the ambient and measured boom levels. Figure 9(b) shows the same data, but where the boom PL values have been replaced by their corresponding values after applying the Butterworth filter. Note that the effective floor is gone and that the p-value has increased many orders of magnitude to 0.322, demonstrating that there is a substantially weaker statistical relationship between ambient and boom PL values (i.e., the fitted slope is much more likely to be equal to zero). Most importantly, the metric values are no longer bounded by the noise measured prior to the boom. Although the range of PL values is much larger after the filtering has been applied, many of these low PL values are associated with sonic booms waveforms with longer rise times and hence less high-frequency energy. It is not

TABLE IV. Statistical descriptions of the distributions shown in Fig. 8.

	Mean (dB)	Standard deviation (dB)
No Filter	3.5	3.1
ISO 11204 (E)	-0.3	1.1
ISO 11204 (F)	0.6	1.4
Butterworth	-0.1	1.4
Brick Wall	-0.3	1.4

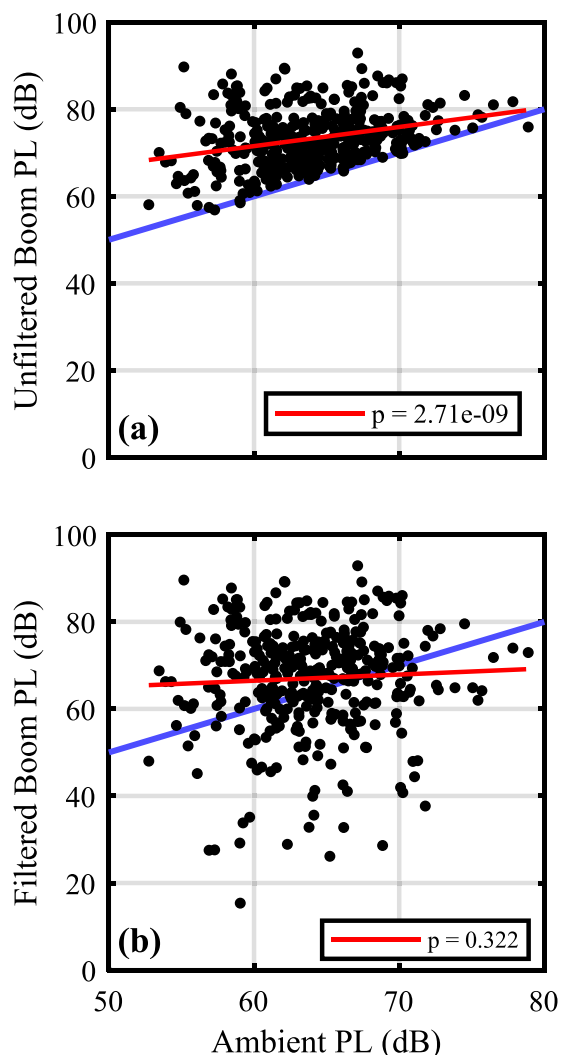


FIG. 9. (Color online) Results of applying the Butterworth filter to the QSF18 dataset. Boom PL is shown as a function of ambient PL, using the 650-ms window immediately before the 650-ms window containing the boom. A total of 379 booms were used: (a) without filtering and (b) after applying the Butterworth filter. The red line indicates the linear fit between the boom and ambient levels and the blue line indicates a one-to-one relationship between levels.

entirely surprising that these sonic booms should have low PL values. However, whether these particularly low metric values truly correspond to human perception remains an open question. It is possible that an end user would choose to simply discard any measurements below a predetermined threshold.

## VII. CONCLUSION

This paper discusses the importance of removing noise contamination in low-boom measurements. The required cutoff frequency for accurate metric calculations is dramatically decreased by applying either a Brick Wall or a sixth-order Butterworth-magnitude filter to the recordings above the frequency at which the SNR drops below 3 dB. Results vary across metrics, but all shown metrics require a cutoff frequency of only 400 Hz or less for accurate calculations

within  $\pm 1$  dB. If no filter is applied, some metrics require a cutoff frequency many times higher, some of which may not even be practically possible in the field.

The Brick Wall and Butterworth filters are successful and robust. Both filters are shown to produce metric calculations that are at least as accurate as the ISO 11204-based method for the test cases shown, even with the Custom E and Custom F corrections.<sup>17</sup> However, for other use cases beyond sonic booms, such as when there is tonal noise or an inconsistent high-frequency roll-off, the ISO 11204 standard may produce better results because it performs a band-by-band correction. In future endeavors, it may be possible to use the Butterworth filter to produce waveforms with reduced high-frequency contaminating noise. All the methods assume stationarity in the contaminating noise, and accuracy will be lost when that assumption is not met.

The two proposed filters, the Brick Wall and Butterworth filters, are straightforward and simple to implement. All the user needs to do is record a short amount of contaminating noise before each boom, calculate the SNR spectrum, and set the filter cutoff frequency to be at the point where the SNR drops below a chosen threshold. Additionally, the Butterworth filter removes the statistical relationship between ambient PL values and sonic boom PL values for measured QSF18 data, indicating that at least the Butterworth method can likely be applied to sonic booms with different shapes than the C609 simulations. The Brick Wall filter's overall success indicates that attempting to perfectly match the high-frequency roll-off of sonic boom spectra is unlikely to yield major improvements. These and other methods should be investigated further when measured low-boom data become available.

## ACKNOWLEDGMENTS

This work was supported by NASA Langley Research Center through National Institute of Aerospace and Analytical Mechanics Associates. Special thanks are given to all those at the NASA Langley Research Center and Brigham Young University who provided feedback on the manuscript. The two anonymous reviewers are also thanked for their prompt and thorough feedback on this manuscript, which led to many meaningful changes to the text and figures. NAVAIR Public Release Distribution Statement A—"Approved for public release; distribution is unlimited" Tracking Number: 2023-88.

## AUTHOR DECLARATIONS

### Conflict of Interest

The authors have no conflict of interest to disclose.

## DATA AVAILABILITY

The data are not available due to security restrictions.

<sup>1</sup>NASA, "NASA Quesst mission webpage," <https://www.nasa.gov/X59/> (2023) (Last viewed June 12, 2024).

- <sup>2</sup>L. P. Ozoroski, G. H. Shah, P. G. Coen, A. Loubeau, and J. Rathsam, "NASA Community Test Workshop 2," NASA Document ID: 20210025956, NASA Langley Research Center (2021).
- <sup>3</sup>J. Rathsam, "An overview of NASA's low boom flight demonstration," *Defense and Aerospace Test and Analysis Workshop Presentation*, NASA Document ID: 20220005452 (2022).
- <sup>4</sup>A. Loubeau and J. Page, "Human perception of sonic boom from supersonic aircraft," *Acoust. Today* **14**(3), 23–30 (2018), available at <https://acousticstoday.org/human-perception-sonic-booms-supersonic-aircraft-alexandra-loubeau-juliet-page/>.
- <sup>5</sup>A. Loubeau, Y. Naka, B. G. Cook, V. W. Sparrow, and J. M. Morgenstern, "A new evaluation of noise metrics for sonic booms using existing data," *AIP Conf. Proc.* **1685**, 090015 (2015).
- <sup>6</sup>A. Loubeau, S. R. Wilson, and J. Rathsam, "Updated evaluation of sonic boom noise metrics," *J. Acoust. Soc. Am.* **144**(1706), 1706 (2018).
- <sup>7</sup>S. S. Stevens, "Perceived level of noise by Mark VII and decibels (*E*)," *J. Acoust. Soc. Am.* **51**(2B), 575–601 (1972).
- <sup>8</sup>K. P. Shepherd and B. M. Sullivan, "A loudness calculation procedure applied to shaped sonic booms," NASA-TP-3134, NASA Langley Research Center (1991).
- <sup>9</sup>J. A. Page, K. K. Hodgdon, P. Krecker, R. Cowart, C. Hobbs, C. Wilmer, C. Koenig, T. Homes, T. Gaugler, D. L. Shumway, J. L. Rosenberger, and D. Philips, "Waveforms and sonic boom perception and response (WSPR): Low-boom community response program pilot test design, execution, and analysis," NASA/CR-2014-218180, NASA Langley Research Center (2014).
- <sup>10</sup>D. J. Maglieri, P. J. Bobbitt, K. J. Plotkin, K. P. Shepherd, P. G. Coen, and D. M. Richwine, "Sonic boom six decades of research," NASA/SP-2014-622, NASA Langley Research Center, Hampton, Virginia (2014).
- <sup>11</sup>J. A. Page, K. K. Hodgdon, R. P. Hunte, D. E. Davis, T. A. Gaugler, R. Downs, R. A. Cowart, D. J. Maglieri, C. Hobbs, G. Baker, M. Collmar, K. A. Bradley, B. Sonak, D. Crom, and C. Cutler, "Quiet supersonic flights 2018 (QSF18) test: Galveston, Texas risk reduction for future community testing with a low-boom flight demonstration vehicle," NASA/CR-2020-220589, NASA Langley Research Center, Hampton, Virginia (2020).
- <sup>12</sup>K. L. Gee, D. J. Novakovich, L. T. Mathews, M. C. Anderson, and R. D. Rasband, "Development of a weather-robust ground-based system for sonic boom measurements," NASA/CR-20205001870, NASA Langley Research Center (2020).
- <sup>13</sup>M. C. Anderson, K. L. Gee, D. J. Novakovich, R. D. Rasband, L. T. Mathews, J. T. Durrant, K. M. Leete, and A. Loubeau, "High-fidelity sonic boom measurements using weather-robust measurement equipment," *Proc. Mtgs. Acoust.* **39**(1), 040005 (2022).
- <sup>14</sup>K. Pedersen, M. K. Transtrum, K. L. Gee, S. V. Lympny, M. M. James, and A. R. Salton, "Validating two geospatial models of continental-scale environmental sound levels," *JASA Express Lett.* **1**, 122401 (2021).
- <sup>15</sup>W. J. Doebler, "Estimated ambient sonic boom metric levels and X-59 signal-to-noise ratios across the USA," *Proc. Mtgs. Acoust.* **42**, 040003 (2020).
- <sup>16</sup>J. Klos, "Recommendations for using noise monitors to estimate noise exposure during X-59 community tests," NASA/TM-20205007926, NASA Langley Research Center, Hampton, Virginia (November, 2020).
- <sup>17</sup>J. Klos, "An adaptation of ISO 11204 using customized correction grades to mitigate ambient noise effects when computing sonic boom loudness levels," NASA/TM-20220010779, NASA Langley Research Center (2022).
- <sup>18</sup>ISO 11204:2010, "Acoustics—Noise emitted by machinery and equipment determination of emission sound pressure levels at a work station and at other specified positions applying accurate environmental corrections" (National Organization for Standardization, Geneva, Switzerland, 2010).
- <sup>19</sup>The MathWorks, Inc., "MATLAB r2022a" (2022).
- <sup>20</sup>S. K. Rallabhandi and A. Loubeau, "Summary of propagation cases of the third AIAA sonic boom prediction workshop," *J. Aircraft* **59**(3), 578–594 (2022).
- <sup>21</sup>W. J. Doebler, S. R. Wilson, A. Loubeau, and V. W. Sparrow, "Simulation and regression modeling of NASA's X-59 low-boom carpets across america," *J. Aircraft* **60**(2), 509–520 (2022).
- <sup>22</sup>M. R. Cook, K. L. Gee, M. K. Transtrum, S. V. Lympny, and M. Calton, "Automatic classification and reduction of wind noise in spectral data," *JASA Express Lett.* **1**(063602), 063602 (2021).